Universität Stuttgart

Fachbereich Mathematik

Multirate time integration for coupled saturated/unsaturated porous medium and free flow systems

Iryna Rybak, Jim Magiera, Rainer Helmig, Christian Rohde

Preprint 2014/016

Fachbereich Mathematik
Fakultät Mathematik und Physik
Universität Stuttgart
Pfaffenwaldring 57
D-70 569 Stuttgart

E-Mail: preprints@mathematik.uni-stuttgart.de
WWW: http://www.mathematik.uni-stuttgart.de/preprints

ISSN **1613-8309**

Multirate time integration for coupled saturated/unsaturated porous medium and free flow systems

Iryna Rybak,[a,*] Jim Magiera,[a] Rainer Helmig,[b] Christian Rohde[a]

[a] *Institute of Applied Analysis and Numerical Simulation, University of Stuttgart, Stuttgart, Germany*

[b] *Institute for Modelling Hydraulic and Environmental Systems, University of Stuttgart, Stuttgart, Germany*

Abstract

A multiple-time-step scheme is developed for solving coupled single-phase free flow and two-fluid-phase porous medium problems. The Stokes equations are applied in the free flow domain, while the Richards equation is used to model saturated/unsaturated porous medium systems. These two flow problems are coupled at the fluid-porous interface via an appropriate set of interface conditions. Numerical simulation results are presented for a model problem and a realistic setting that demonstrate the convergence and efficiency of the proposed computational algorithm. Time-splitting multistep methods can be successfully applied for modeling other physical systems where the processes evolve on different time scales, and these potential extensions are discussed.

Key words: Free flow, Porous medium, Coupling, Stokes equations, Richards equation, Interface conditions, Multiple-time-step method

* Corresponding author

Email addresses: rybak@ians.uni-stuttgart.de (Iryna Rybak,), magierjm@mathematik.uni-stuttgart.de (Jim Magiera,), rainer.helmig@iws.uni-stuttgart.de (Rainer Helmig,), crohde@mathematik.uni-stuttgart.de (Christian Rohde).

26 August 2014

1 Introduction

Coupled unsaturated porous medium and free flow systems appear routinely in environmental settings such as evaporation from soil influenced by wind, overland flow interactions with groundwater aquifers, salt precipitation in drying porous media, surface water and groundwater contamination. These flow systems contain different sets of entities (pure fluid in the free flow domain, fluids and solid in the porous medium region) that require a separate model for each flow system and an accurate coupling of these models at the interface between the systems [24]. In addition, physical processes in these systems often evolve on different scales in time (fluid velocity in the free flow region is usually much higher than the velocity of fluids through porous media). This fact should be taken into account while developing effective numerical algorithms for solving such coupled problems.

In the free flow domain, the (Navier–)Stokes equations are usually applied to describe momentum conservation, while Darcy's law is considered as an approximation of momentum conservation in the porous medium. To couple these flow systems, in addition to mass conservation and balance of normal forces across the fluid-porous interface, the Beavers–Joseph velocity jump condition [1] is often considered. This condition provides the connection between the free flow velocity and the porous medium velocity tangential to the interface. Other interface conditions are possible [18].

Mathematical models and numerical algorithms for solving such coupled flow problems have been developed and analyzed during the last decade mainly for stationary single-fluid-phase systems [8, 9, 20] that describe steady-state interactions between the free flow and saturated porous media. The models usually contain coupled stationary Stokes/Darcy or Navier–Stokes/Darcy equations. Recent advances in numerical methods for coupled non-stationary single-phase Stokes/Darcy systems are presented in [4, 5, 13, 14, 17, 27], where the same time step is applied in both flow domains. A new coupling concept for a compositional single-phase free flow and compositional two-fluid-phase porous medium systems is proposed in [16], where the non-stationary problem is solved using the monolithic approach.

To solve coupled multiphysics problems effectively, partitioning schemes are often applied. Decoupled algorithms for steady-state, single-phase free and porous medium flow problems are based on iterative domain decomposition methods [3,8,9], while for non-stationary flow problems non-iterative splitting schemes are usually applied [6,13,14]. For many applications the fluid velocity in the free flow region is much higher than that through the porous medium. In this case, it is reasonable to apply a multiple-time-step technique: to compute fast/slow solutions using a small/large time step.

First results on multistep methods for single-phase Stokes/Darcy problem are presented in [23], where a decoupled scheme is proposed and the stability of the numerical algorithm for a finite time interval is proved. However, the considered scheme is not mass conservative across the interface. In [21], a mass conservative multiple-time-step algorithm for the Stokes/Darcy system is developed and the long time stability of the numerical method is proved. Several partitioning schemes for non-stationary single-fluid-phase Stokes/Darcy problems are compared in [22].

A wide range of applications, such as river or lake interactions with the vadose zone, evaporation from soil systems influenced by wind, and precipitation of salts in drying porous media, requires multiphase physics in the subsurface. In this case, the porous medium model typically includes multiphase Darcy's law or Richards' equation. Multiphase Darcy's law represents flows of several fluids while Richards' equation [19] describes movement of only water through saturated/unsaturated porous media. The latter case is however sufficient to adequately describe many of the applications.

Coupling of subsurface flows described by Richards' equation and overland flows has been studied intensively in the last decade. There are several possible models for the surface flows, starting from the Navier–Stokes equations and ending with considering source terms at the fluid-porous interface that represent, e.g., the rainfall rate and play a role of boundary conditions for the subsurface flow model. Coupling shallow water equations and Richards' equation is considered in [7]. More simple models such as a kinematic wave equation or a diffusion wave approximation of the Saint–Venant equation [12, 26], or even ODE for modeling surface runoff [2] coupled with the Richards equation are investigated.

A multiple-time-stepping scheme for coupled kinematic wave equation and Richards' equation is proposed in [25]. Up to our knowledge, there are no results available in the literature for coupling the Stokes and Richards equations. Therefore, the main objective of the present work is to develop a multistep splitting scheme for the Stokes/Richards problem to efficiently simulate overland flow interactions with saturated/unsaturated groundwater flows.

The paper is organized as follows. The flow system of interest, the flow models, and the corresponding interface conditions are described in section 2. The decoupled multiple-time-step scheme is presented in section 3. The numerical simulation results that include the convergence study of the proposed method and demonstrate the advantage of the multirate time integration for modeling such multiphysical systems are presented in section 4. Finally, possible extensions of this work are discussed.

2 Flow system description

The system of interest contains a free flow domain Ω_{ff} filled with a single fluid phase (water) and a porous medium Ω_{pm} composed of two fluid phases (air, water) and a solid phase (Fig. 1). The flow regions are separated by a sharp interface Γ which cannot store and transfer mass, momentum, and energy [10].

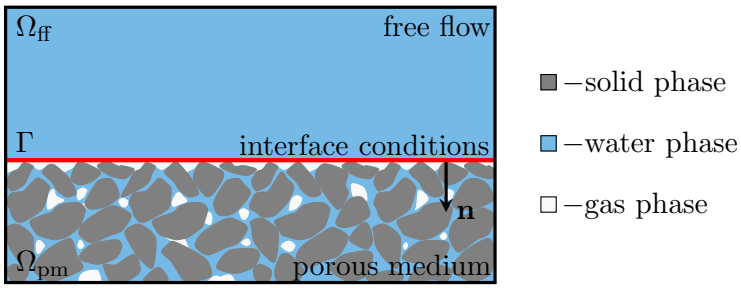

Fig. 1. Schematic representation of the coupled single-phase free flow and two-fluid-phase porous medium systems.

We deal with isothermal processes and assume that the fluids are incompressible and the solid is rigid. The primary application of interest in this work is infiltration of water into an unsaturated soil system.

2.1 Free flow model

The mass conservation equation for incompressible fluids reads

$$\nabla \cdot \mathbf{v} = 0 \qquad \text{in } \Omega_{\text{ff}} \times (0, T], \tag{1}$$

where $\mathbf{v}$ is the fluid velocity, and $T > 0$ is the final time.

Considering laminar flows and neglecting the inertial term, the momentum balance reduces to the Stokes equations

$$\rho \frac{\partial \mathbf{v}}{\partial t} - \nabla \cdot \mathbf{T}(\mathbf{v}, p) - \rho \mathbf{g} = 0 \qquad \text{in } \Omega_{\text{ff}} \times (0, T], \tag{2}$$

where ρ is the fluid density, $\mathbf{T}(\mathbf{v}, p) = 2\mu \mathbf{D}(\mathbf{v}) - p\mathbf{I}$ is the stress tensor, μ is the dynamic viscosity, p is the fluid pressure, $\mathbf{D}(\mathbf{v}) = \frac{1}{2}\left(\nabla \mathbf{v} + (\nabla \mathbf{v})^{\mathrm{T}}\right)$ is the rate of strain tensor, $\mathbf{I}$ is the identity tensor, and $\mathbf{g}$ is the gravitational acceleration. Further, we will define $\mathbf{f}_{\text{ff}} := \rho \mathbf{g}$, and move it to the right-hand side.

The model problem (1)–(2) is subject to the initial data

$$\mathbf{v}(\mathbf{x}, 0) = \mathbf{v}_0(\mathbf{x}) \qquad \text{in } \overline{\Omega}_{\text{ff}}, \tag{3}$$

the interface conditions on Γ, which will be specified later on, and the boundary conditions at the external boundary $\partial\Omega_{\text{ff}} \setminus \Gamma$ of the free flow domain

$$\begin{aligned} \mathbf{v} &= \mathbf{v}_D \qquad \text{on } \partial\Omega_{\text{ff},D} \times (0,T], \\ \mathbf{T}(\mathbf{v}, p)\cdot\mathbf{n} &= \mathbf{v}_N \qquad \text{on } \partial\Omega_{\text{ff},N} \times (0,T], \end{aligned} \tag{4}$$

where $\partial\Omega_{\text{ff},D}$ is the part of the external boundary with Dirichlet boundary conditions, and $\partial\Omega_{\text{ff},N}$ is the part of the boundary with Neumann boundary conditions such that $\partial\Omega_{\text{ff}} = \partial\Omega_{\text{ff},D} \cup \partial\Omega_{\text{ff},N} \cup \Gamma$. The primary variables for the free flow model are $\mathbf{v}$ and p.

2.2 Porous medium model

Due to differences in the properties between air and water, it is possible to simplify the general two-fluid-phase porous medium equations. Air is much more mobile than water, and thus can move easily with a very small pressure gradient which can be neglected. This is the basis for the Richards assumption. Therefore, many unsaturated porous medium systems can be described by the Richards equation, which is a combination of the mass conservation equation for the water phase

$$\phi\frac{\partial S_w}{\partial t} + \nabla\cdot\mathbf{v}_w = f_{\text{pm}} \qquad \text{in } \Omega_{\text{pm}} \times (0,T], \tag{5}$$

and the generalized Darcy's law

$$\mathbf{v}_w = -\frac{\mathbf{K}k_{rw}}{\mu_w}(\nabla p_w - \rho_w\mathbf{g}) \qquad \text{in } \Omega_{\text{pm}} \times (0,T]. \tag{6}$$

Here $\mathbf{v}_w$ is the velocity of water through porous media, ϕ is the porosity, S_w is the water-phase saturation, $\mathbf{K}$ is the intrinsic permeability tensor, $k_{rw} = k_r(S_w)$ is the relative permeability which is a given function of the water-phase saturation, p_w is the pressure of the water phase, μ_w is the dynamic viscosity, ρ_w is the density of water, and f_{pm} is the source/sink term.

The air-phase pressure p_a is assumed to be equal to the atmospheric pressure. We will use a reference pressure equal to the atmospheric pressure such that $p_a = 0$. Therefore, the capillary pressure p_c, which is also a known function of the water-phase saturation, becomes equal to the opposite of the water-phase pressure, $p_c(S_w) = p_a - p_w = -p_w$. The primary variable of the porous medium model is the water-phase pressure. Since we model the properties of the water phase only, the subscript w will be omitted for convenience.

Substitution of Darcy's law (6) into the mass conservation equation (5) yields the pressure based formulation which is the Richards equation

$$\phi \frac{\partial S}{\partial t} - \nabla \cdot \left(\frac{\mathbf{K} k_r}{\mu} \left(\nabla p - \rho \mathbf{g} \right) \right) = 0 \quad \text{in } \Omega_{\text{pm}} \times (0, T]. \tag{7}$$

Equation (7) is nonlinear due to the relationships between pressure and saturation, $p = -p_c(S)$, and between relative permeability and saturation, $k_r = k_r(S)$. In the saturated zone, we have $S = 1$ and $k_r = 1$. Therefore, in this region, $\Omega_{\text{pm,sat}} \subset \Omega_{\text{pm}}$, equation (7) reduces to the steady-state single-phase porous medium model

$$-\nabla \cdot \left(\frac{\mathbf{K}}{\mu} \left(\nabla p - \rho \mathbf{g} \right) \right) = 0 \qquad \text{in } \Omega_{\text{pm,sat}} \times (0, T]. \tag{8}$$

The general porous medium model (7) has to be supplemented by the appropriate set of the initial conditions

$$p(\mathbf{x}, 0) = p_0(\mathbf{x}) \qquad \text{in } \overline{\Omega}_{\text{pm}}, \tag{9}$$

the interface conditions on Γ, which will be described in the next section, and the boundary conditions on the external boundary of the porous medium domain

$$\begin{aligned} p &= p_D \qquad \text{on } \partial\Omega_{\text{pm},D} \times (0, T], \\ \mathbf{v} \cdot \mathbf{n} &= p_N \qquad \text{on } \partial\Omega_{\text{pm},N} \times (0, T], \end{aligned} \tag{10}$$

where $\partial\Omega_{\text{pm}} = \partial\Omega_{\text{pm},D} \cup \partial\Omega_{\text{pm},N} \cup \Gamma$.

2.3 Interface conditions

In addition to the boundary conditions prescribed on the external boundary of the coupled domain, interface conditions have to be defined on the fluid-porous interface Γ. The superscripts ff and pm determine the free flow and the porous medium quantities, respectively.

The *conservation of mass* across the interface requires the mass flux leaving the free flow domain to be equal to the mass flux entering the porous medium. Since only the water-phase dynamics is modeled in the subsurface, we can write

$$\left[\mathbf{v} \cdot \mathbf{n} \right]^{\text{ff}} = - \left[\mathbf{v} \cdot \mathbf{n} \right]^{\text{pm}} \qquad \text{on } \Gamma \times (0, T], \tag{11}$$

where $\mathbf{n}$ is the unit normal vector outward from the free flow domain at the interface (Fig. 1) such that $\mathbf{n}^{\text{ff}} = \mathbf{n}$, and $\mathbf{n}^{\text{pm}} = -\mathbf{n}$.

The normal stress for Newtonian fluids at the interface from the free flow side is given by $\left[\mathbf{n} \cdot \mathbf{T} \left(\mathbf{v}, p \right) \cdot \mathbf{n} \right]^{\text{ff}} = \left[\mathbf{n} \cdot \left(2\mu \mathbf{D} \left(\mathbf{v} \right) - p\mathbf{I} \right) \cdot \mathbf{n} \right]^{\text{ff}}$. In the porous medium,

slow flow is assumed and Darcy's law is used, thus viscous stress is not treated explicitly, it is already accounted for in the permeability. Therefore, pressure is the only force acting on the interface that has to be taken into account from the porous medium domain $[\mathbf{n}\cdot\mathbf{T}(\mathbf{v},p)\cdot\mathbf{n}]^{\mathrm{pm}} = -p^{\mathrm{pm}}$. Under the assumption of a rigid solid, the normal stress of the solid phase at the interface can be considered as opposite to the water-phase pressure. We also assume that the normal stress for the air phase at the interface is opposite to the water-phase pressure. Therefore, the *balance of normal forces* across the interface can be formulated as

$$[\mathbf{n}\cdot\mathbf{T}(\mathbf{v},p)\cdot\mathbf{n}]^{\mathrm{ff}} = -p^{\mathrm{pm}} \qquad \text{on } \Gamma\times(0,T]. \tag{12}$$

The *Beavers–Joseph–Saffman* interface condition [1] for the tangential components of the free flow velocity is given by

$$\left[\mathbf{v}\cdot\boldsymbol{\tau}_i + \frac{2\sqrt{\mathbf{K}}}{\alpha_{\mathrm{BJ}}}\mathbf{n}\cdot\mathbf{D}(\mathbf{v})\cdot\boldsymbol{\tau}_i\right]^{\mathrm{ff}} = 0, \quad i = 1,...,d-1, \tag{13}$$

on $\Gamma\times(0,T]$, where $\alpha_{\mathrm{BJ}} > 0$ is the Beavers–Joseph parameter, $\boldsymbol{\tau}$ is the unit vector tangential to the interface, and d is the number of space dimensions.

3 Numerical scheme

For solving multiphysics problems, where the processes evolve on different time scales, application of decoupled schemes with different time steps in the subdomains pays off. For the majority of applications, the free flow velocity is much higher than the fluid velocity through a porous medium. Therefore, it is efficient to compute the fast (free flow) solutions on a fine mesh in time and the slow (porous medium) solutions on a coarse mesh in time.

Different decoupled algorithms can be developed: the free flow problem is solved first at the coarse time interval and after that the porous medium problem is computed (Fig. 2) or vice versa. Coupling mechanisms at the common time levels t_{m_k} (Fig. 2) can also be different, e.g., the last value computed on the fine mesh is transferred to the slow process or an average of the fast solution over the coarse time interval is considered. Different time partitioning schemes for the Stokes/Darcy problem are considered in [21–23]. In this work, we study the algorithm schematically presented in Fig. 2 to solve the Stokes/Richards problem.

3.1 Time splitting

We introduce two grids in time: the fine grid with a small step $\Delta t > 0$ on which the free flow solutions are computed $\{t_m = m\Delta t,\ m = 0, \dots, Mr\}$, and the coarse grid $\{t_{m_k} = k\Delta T,\ k = 0, \dots, M\}$ for the porous medium solutions, where $\Delta T = r\Delta t$, and $r > 0$ is the ratio between the fine and coarse time steps. The flow problems are coupled at the coarse time levels t_{m_k} (Fig. 2).

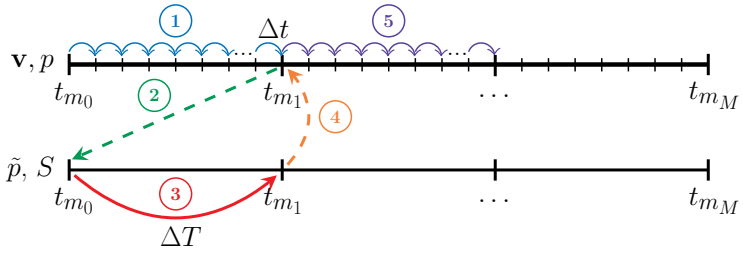

Fig. 2. Decoupled multiple-time-step scheme (free flow - top, porous medium - bottom).

For convenience we redefine the water-phase pressure in the porous medium as $\tilde{p}$ and denote discrete analogues of the primary variables in two flow domains as $\mathbf{v}_h^m$, p_h^m, and $\tilde{p}_h^{m_k}$. We introduce the space discretization operators $\mathrm{D_{ff}}$ and $\mathrm{A_{ff}}$ for the free flow equations (1) and (2), respectively, and the operator $\mathrm{A_{pm}}$ for the porous medium problem (7). The operator $\mathrm{A_{ffpm}}$ discretizes the coupling conditions (12)–(13) which serve as boundary conditions for the free flow domain, and the operator $\mathrm{A_{pmff}}$ stands for the interface condition (11) which is used as the boundary condition for the porous medium region.

Algorithm 1 (Multistep Stokes/Richards scheme)

for $k = 0$ **to** $M - 1$ **do**

for $m = m_k$ **to** $m_{k+1} - 1$ **do**

$$\rho \frac{\mathbf{v}_h^{m+1} - \mathbf{v}_h^m}{\Delta t} + \mathrm{A_{ff}}\left(\mathbf{v}_h^{m+1}, p_h^{m+1}\right) + \mathrm{A_{ffpm}}\left(\mathbf{v}_h^{m+1}, p_h^{m+1}, \tilde{p}_h^{m_k}\right) = \mathbf{f}_{\mathrm{ff}}^{m+1}$$
$$\mathrm{D_{ff}}\left(\mathbf{v}_h^{m+1}\right) = 0$$

end for

$$\phi \frac{S\left(\tilde{p}_h^{m_{k+1}}\right) - S\left(\tilde{p}_h^{m_k}\right)}{\Delta T} + \mathrm{A_{pm}}\left(\tilde{p}_h^{m_{k+1}}\right) + \mathrm{A_{pmff}}\left(\mathbf{v}_h^{m_{k+1}}, \tilde{p}_h^{m_{k+1}}\right) = f_{\mathrm{pm}}^{m_{k+1}}$$

end for

The definition of the space discretization operators can be found in section 3.2. In both flow domains, the implicit Euler schemes are applied. The decoupled

multistep Stokes/Richards algorithm schematically presented in Fig. 2 can be formulated using the above notations as follows.

3.2 Space discretization

The finite volume method on staggered grids [28] is considered as the space discretization in both flow domains. Such a choice allows to avoid spurious oscillations in the free flow domain without applying any stabilization technique. The computational domains $\Omega_{\rm ff}$ and $\Omega_{\rm pm}$ are partitioned into equal blocks of size $h_x \times h_y$ (Fig. 3, dashed lines), and the grids are conforming at the interface Γ. The fluid pressures are computed in the centers of the blocks (x_i, y_j), where $x_i = (i + 0.5)h_x$, $y_j = (j + 0.5)h_y$, $i = 0, \ldots, N_x$, $j = 0, \ldots, N_y$. In addition, the porous medium pressure is computed at the fluid-porous interface and at the external boundary of the porous medium domain.

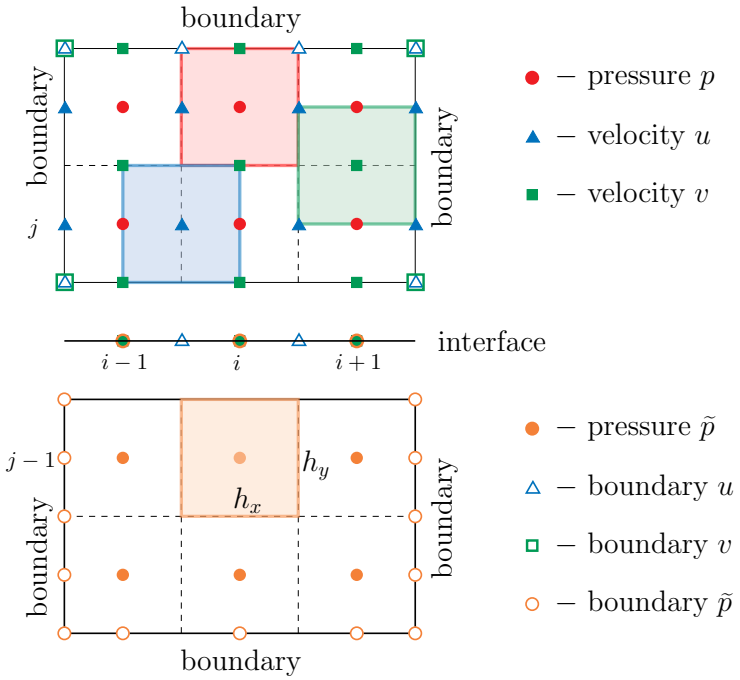

Fig. 3. Staggered grid in the coupled domain (free flow - top, porous medium - bottom).

The fluid velocities $\mathbf{v} = (u, v)$ are computed in the centers of the block faces and additionally at the interface and the external boundary. As a consequence, different control volumes are considered for different variables (staggered grid, Fig. 3). In the porous medium domain, velocities are not the primary variables, and thus are computed at the post-processing stage.

3.2.1 *Free flow discretization*

For completeness of the discrete problem formulation, we briefly describe the discretization schemes in both flow domains and the coupling at the fluid-porous interface. For simplicity of notation, we omit the time levels for the space discretization operators and mark the grid nodes according to Fig. 4, where P is the center of the corresponding control volume.

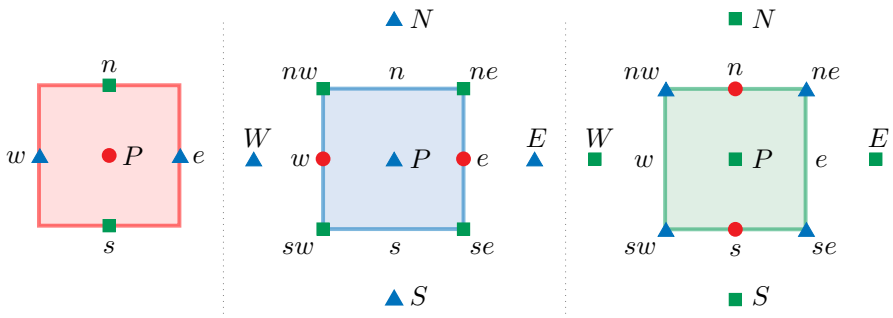

Fig. 4. Control volumes for the free flow primary variables: p (left), u (middle), and v (right).

Integrating the mass balance equation (1) over the corresponding control volume (Fig. 4, left), we get

$$(u_e - u_w)\, h_y + (v_n - v_s)\, h_x = 0, \tag{14}$$

and the discrete divergence operator D_{ff} is defined as

$$\mathrm{D}_{\mathrm{ff}}\left(\mathbf{v}_h\right) = \left(u_e - u_w\right)/h_x + \left(v_n - v_s\right)/h_y.$$

The space approximation $\mathrm{A}_{\mathrm{ff}}\left(\mathbf{v}_h, p_h\right)$ of the momentum balance equation (2) contains the horizontal component $\mathrm{A}^u_{\mathrm{ff}}$ and the vertical component $\mathrm{A}^v_{\mathrm{ff}}$. The horizontal component can be written for the corresponding inner control volume (Fig. 4, middle) as follows

$$\mathrm{A}^u_{\mathrm{ff}} = \left(F^u_{x,e} - F^u_{x,w}\right)/h_x + \left(F^u_{y,n} - F^u_{y,s}\right)/h_y, \tag{15}$$

where the momentum fluxes are defined as

$$F^u_{x,e} = p_e - 2\mu_e \frac{u_E - u_P}{h_x}, \quad F^u_{x,w} = p_w - 2\mu_w \frac{u_P - u_W}{h_x},$$

$$F^u_{y,n} = -\mu_n \left(\frac{u_N - u_P}{h_y} + \frac{v_{ne} - v_{nw}}{h_x}\right), \quad F^u_{y,s} = -\mu_s \left(\frac{u_P - u_S}{h_y} + \frac{v_{se} - v_{sw}}{h_x}\right).$$

When the control volume lies on the left or right boundary and Neumann boundary conditions are prescribed there, the integration is performed over the half volume and the given flux enters the right-hand side of the resulting system of linear equations. In case of Dirichlet boundary conditions on the

left/right boundary, the corresponding velocity values are incorporated into the right-hand side of the resulting system of linear equations. For control volumes lying on the top boundary or at the interface, one-sided differences with half-step size are applied to approximate the corresponding fluxes, e.g.,

$$F^u_{y,n} = -\mu_n \left(\frac{u_n - u_P}{0.5 h_y} + \frac{v_{ne} - v_{nw}}{h_x} \right).$$

In the same way we obtain the space approximation for the vertical component of the momentum conservation in the corresponding control volume (Fig. 4, right):

$$\mathrm{A}^v_{\mathrm{ff}} = \left(F^v_{x,e} - F^v_{x,w} \right) / h_x + \left(F^v_{y,n} - F^v_{y,s} \right) / h_y, \tag{16}$$

where the fluxes across the finite volume edges are defined for the inner control volumes as

$$F^v_{x,e} = -\mu_e \left(\frac{u_{ne} - u_{se}}{h_y} + \frac{v_E - v_P}{h_x} \right), \quad F^v_{x,w} = -\mu_w \left(\frac{u_{nw} - u_{sw}}{h_y} + \frac{v_P - v_W}{h_x} \right),$$
$$F^v_{y,n} = p_n - 2\mu_n \frac{v_N - v_P}{h_y}, \quad F^v_{y,s} = p_s - 2\mu_s \frac{v_P - v_S}{h_y}.$$

Control volumes on the top boundary and interface are half smaller than the inner control volumes and are treated accordingly.

The finite volume scheme based on discretizations (14)–(16) is locally mass conservative and does not require any stabilization for the pressure. The approximation is of second order in space for inner control volumes, and second or first order near the boundary depending on the boundary conditions. However, due to smaller space steps for the boundary control volumes the error in the latter case is reduced. More details on space discretizations can be found in [28, chap. 6.2–6.3].

3.2.2 Porous medium discretization

In the porous medium domain, the pressure is the primary variable. The space discretization operator A_{pm} for inner control volumes is defined as

$$\mathrm{A}_{\mathrm{pm}}\left(\widetilde{p}_h\right) = \left(\widetilde{u}_e - \widetilde{u}_w\right) / h_x + \left(\widetilde{v}_n - \widetilde{v}_s\right) / h_y, \tag{17}$$

where the velocities are approximated at the cell boundaries by the central differences, and the upwind scheme is applied for the gravity-driven advection terms

$$\widetilde{u}_e = -\frac{k_{xx,e}}{\mu_e} \frac{k_{\mathrm{rel}}\left(S\left(\widetilde{p}_P\right)\right) + k_{\mathrm{rel}}\left(S\left(\widetilde{p}_E\right)\right)}{2} \frac{\widetilde{p}_E - \widetilde{p}_P}{h_x},$$
$$\widetilde{u}_w = -\frac{k_{xx,w}}{\mu_w} \frac{k_{\mathrm{rel}}\left(S\left(\widetilde{p}_P\right)\right) + k_{\mathrm{rel}}\left(S\left(\widetilde{p}_W\right)\right)}{2} \frac{\widetilde{p}_P - \widetilde{p}_W}{h_x},$$

$$\widetilde{v}_n = -\frac{k_{yy,n}}{\mu_n}\frac{k_{\mathrm{rel}}\left(S\left(\widetilde{p}_N\right)\right)+k_{\mathrm{rel}}\left(S\left(\widetilde{p}_P\right)\right)}{2}\frac{\widetilde{p}_N-\widetilde{p}_P}{h_y}-\frac{k_{yy,n}k_{\mathrm{rel}}\left(S\left(\widetilde{p}_N\right)\right)}{\mu_n}\rho_n g,$$
$$\widetilde{v}_s = -\frac{k_{yy,s}}{\mu_s}\frac{k_{\mathrm{rel}}\left(S\left(\widetilde{p}_P\right)\right)+k_{\mathrm{rel}}\left(S\left(\widetilde{p}_S\right)\right)}{2}\frac{\widetilde{p}_P-\widetilde{p}_S}{h_y}-\frac{k_{yy,s}k_{\mathrm{rel}}\left(S\left(\widetilde{p}_P\right)\right)}{\mu_s}\rho_s g.$$

Here, the intrinsic permeability tensor is assumed to be diagonal $\mathbf{K} = \mathrm{diag}\left(k_{xx}, k_{yy}\right)$, and the grid nodes are chosen according to Fig. 5.

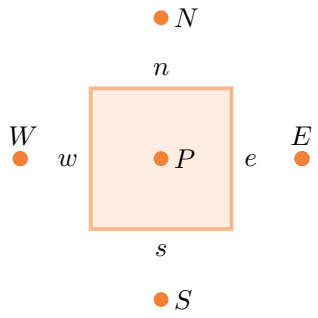

Fig. 5. Control volume for the porous medium pressure $\widetilde{p}$.

Due to the functional dependencies between the pressure and saturation, and between the relative permeability and saturation, the porous medium problem is nonlinear. The Newton method is applied to solve it.

Let $\mathcal{I}$ be the index set of all degrees of freedom for the subsurface domain. At each time level $t_{m_{k+1}}$, the following nonlinear system of equations

$$\mathbf{F}\left(\widetilde{p}^{m_{k+1}}, \widetilde{p}^{m_k}\right) = 0 \tag{18}$$

is solved for the given $\widetilde{p}^{m_k}$, where

$$\mathbf{F}\left(\widetilde{p}^{m_{k+1}}, \widetilde{p}^{m_k}\right) = \left[F_{ij}\left(\widetilde{p}^{m_{k+1}}, \widetilde{p}^{m_k}\right)\right]_{ij\in\mathcal{I}},$$

and for each inner node

$$F_{ij} \coloneqq \phi\frac{S\left(\widetilde{p}_P^{m_{k+1}}\right)-S\left(\widetilde{p}_P^{m_k}\right)}{\Delta T}+\frac{\widetilde{u}_e^{m_{k+1}}-\widetilde{u}_w^{m_{k+1}}}{h_x}+\frac{\widetilde{v}_n^{m_{k+1}}-\widetilde{v}_s^{m_{k+1}}}{h_y}.$$

The time step ΔT is regulated adaptively according to the number of the Newton iterations.

On the boundary, we distinguish between the Dirichlet boundary nodes

$$F_{ij} \coloneqq p_P - p_{\mathrm{D}}(\mathbf{x}_P),$$

and the Neumann boundary nodes

$$F_{ij} \coloneqq \mathbf{v}\left(p_P, p_Q\right)\cdot\mathbf{n} - p_N(\mathbf{x}_P),$$

where $\mathbf{x}_Q$ are the coordinates of the point $Q \in \mathcal{I}$, and $\mathbf{v}\left(p_P, p_Q\right)$ is an approximation of the fluid velocity at the node P using neighbouring nodes Q.

The nonlinear system (18) is solved by a Jacobian-explicit Newton scheme using the NOX package of the Trilinos framework [11]. For the resulting system of linear equations the direct solver SuperLU [15] is applied.

3.2.3 Coupling of flow domains

The mass conservation across Γ given by the interface condition (11) is approximated as

$$v_P = -\frac{k_{yy,P} k_{\mathrm{rel}}\left(S\left(\widetilde{p}_P\right)\right)}{\mu_P}\left[\frac{\widetilde{p}_s - \widetilde{p}_P}{0.5 h_y} + \rho_P g\right], \tag{19}$$

where the stencil of the scheme is presented in Fig. 6.

Discretization of the balance of normal forces (12) is written in the following way

$$p_n - 2\mu_n \frac{v_N - v_P}{h_y} = \widetilde{p}_P. \tag{20}$$

The Beavers–Joseph condition (13) is approximated as

$$u_w + \frac{\sqrt{k_{xx}}}{\alpha_{\mathrm{BJ}}}\left(\frac{u_{nw} - u_w}{0.5 h_y} + \frac{v_P - v_W}{h_x}\right) = 0. \tag{21}$$

The flow systems are not coupled at the two corner points where the interface meets the boundary (nodes BC, Fig. 6). At these nodes, the boundary conditions are specified.

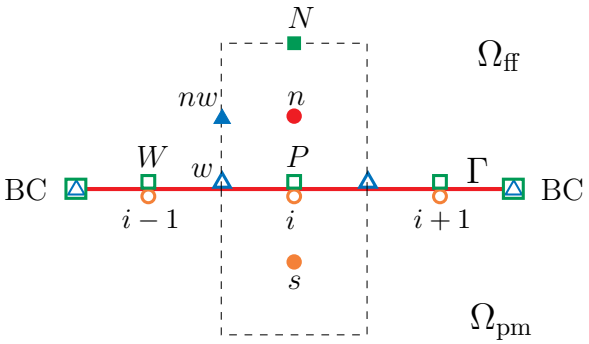

Fig. 6. Grid nodes for the interface conditions.

4 Numerical simulations

In this section, we present numerical simulation results for two problems. First, we test the algorithm for a model problem where the exact solutions in both flow domains are chosen such that the interface conditions are satisfied, and the relationships between the relative permeability and saturation, and between the capillary pressure and saturation are reasonable. We perform the numerical convergence study of the splitting algorithm and evaluate the speedup of computations for different ratios between the time steps. Then, we study the effectivity of the numerical scheme for a realistic example.

4.1 Model problem

We consider the flow domains $\Omega_{\rm ff} = [0,1] \times [1,2]$ and $\Omega_{\rm pm} = [0,1] \times [0,1]$ with the interface $\Gamma = (0,1) \times \{1\}$, and choose the model parameters $\phi = 1$, $\rho = 1$, $\mu = 1$, $\alpha_{\rm BJ} = 1$, $\mathbf{K} = \mathbf{I}$, $\mathbf{g} = \mathbf{0}$. We apply the following relationships between the relative permeability and saturation $k_r(S) = S^2$, and between the capillary pressure and saturation $p_c(S) = -S$. The exact solution which satisfies the interface conditions (11)-(13) is chosen as follows

$$\begin{aligned} u(x,y,t) &= -\cos(\pi x)\sin(\pi y)\exp(t), \\ v(x,y,t) &= \sin(\pi x)\cos(\pi y)\exp(t), \\ p(x,y,t) &= \sin^{\frac{1}{3}}(\pi x)\, y^2 \exp(t), \\ \widetilde{p}(x,y,t) &= \sin^{\frac{1}{3}}(\pi x)\, y \exp(t). \end{aligned} \tag{22}$$

The right-hand sides and the corresponding initial and boundary conditions are defined by substitution of the parameters and the exact solution (22) into the problem formulation (1)-(10). We consider Dirichlet boundary conditions at the external boundary of the domain.

For the computations we apply the decoupled scheme described in Algorithm 1 with the same time steps in both subdomains ($r = 1$) and with a larger time step in the porous medium using different ratios r between the time steps. We consider five levels of grid refinement starting from $h_x = h_y = h = 0.2$ and $\Delta t = 0.04$ and decreasing the space step by a factor of two and time step by a factor of four. For all the primary variables we compute the relative errors $\varepsilon_f = \|f - f_h\|_{L^2} / \|f\|_{L^2}$, where $f \in \{u, v, p, \widetilde{p}\}$.

The numerical simulation results are presented in Fig. 7 for the free flow and porous medium solutions. These results demonstrate second order convergence in space and first order in time for different ratios r between the time steps applied in Algorithm 1. The multiple-time-step schemes ($r = 5$ and $r = 10$) are

slightly less accurate in comparison with that of the single-time-step algorithm ($r = 1$) due to larger time steps used in the porous medium domain ($\Delta T = r\Delta t$). However, the errors are of the same order of magnitude, and all the schemes exhibit the same convergence order in space and time. In addition, the multirate schemes are much faster.

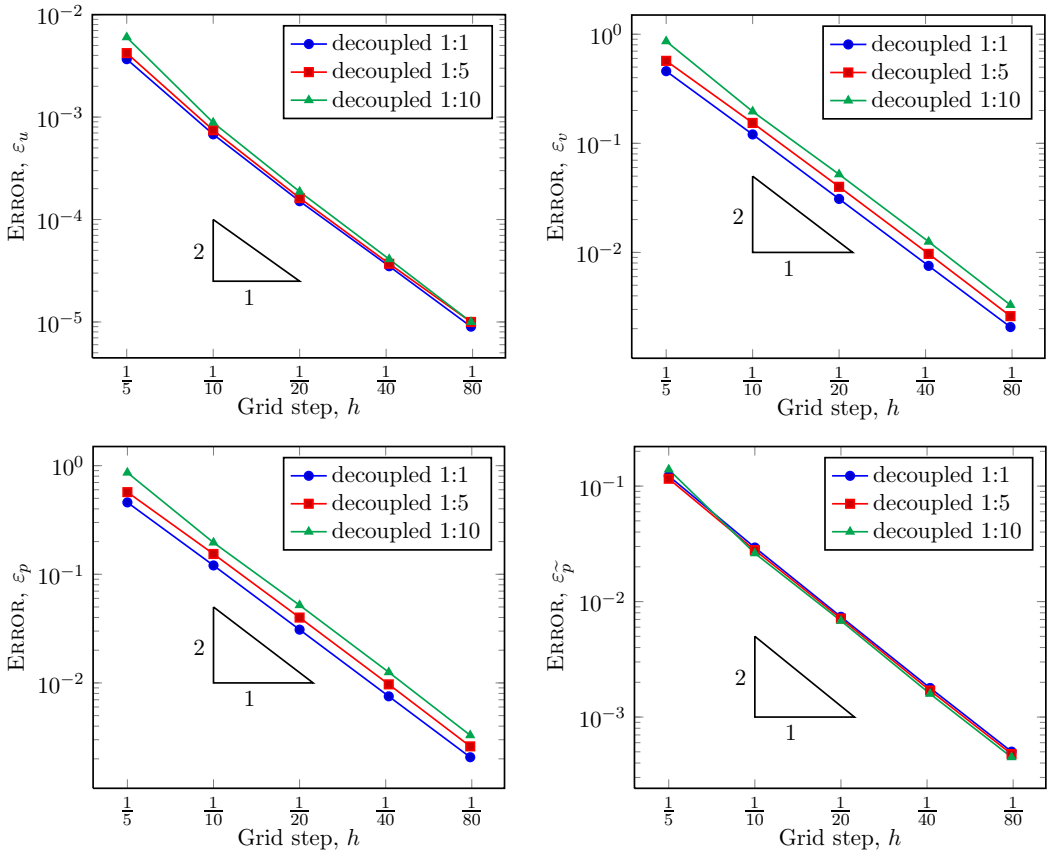

Fig. 7. Error analysis for Algorithm 1 (free flow and porous medium solutions), time step ratio $1 : r$.

To demonstrate the advantage of the multirate time integration, we run simulations using Algorithm 1 for $T = 1$ and compare computational times needed for solving the coupled flow problem applying different ratios between the time steps in the free flow and porous medium domains. For the numerical simulations we consider $h_x = h_y = h = 2.5 \cdot 10^{-2}$ and $\Delta t = 6.25 \cdot 10^{-4}$. The preassigned tolerance for the Newton method is taken $\varepsilon_{\text{tol}} = 10^{-10}$.

In Table 1, we present the CPU times spent on solving the coupled flow problem for different ratios r, and determine the speedup of the computations.

$$\text{Speedup} = \frac{\text{CPU time for } r = i}{\text{CPU time for } r = 1}, \; i = 1,\, 2,\, 5,\, 10,\, 20,\, 30.$$

Ratio r	1	2	5	10	20	30
CPU time, [s]	150.2	77.1	36.7	21.2	11.8	8.6
Speedup	1	1.9	4.1	7.1	12.7	17.5

Table 1
Speedup of Algorithm 1 for different time step ratios (model problem).

The results presented in Table 1 demonstrate the effectivity of applying the multirate time-splitting scheme given in Algorithm 1 for solving the coupled flow problem (1)–(10).

4.2 Realistic example

Consider $\Omega_{\text{ff}} = [0, 4\text{m}] \times [1, 2\text{m}]$, $\Omega_{\text{pm}} = [0, 4\text{m}] \times [0, 1\text{m}]$, and $\Gamma = (0, 4\text{m}) \times \{1\text{m}\}$. The fluid is water with density $\rho = 10^3\,[\text{kg/m}^3]$ and dynamic viscosity $\mu = 8.9 \times 10^{-4}\,[\text{Pa s}]$. The soil is isotropic with permeability $k_{xx} = k_{yy} = 5 \cdot 10^{-8}\,[\text{m}^2]$ and porosity $\phi = 0.38$. The Beavers–Joseph coefficient is $\alpha_{\text{BJ}} = 1$. Gravitational effects are neglected $\mathbf{g} = (0, 0)$.

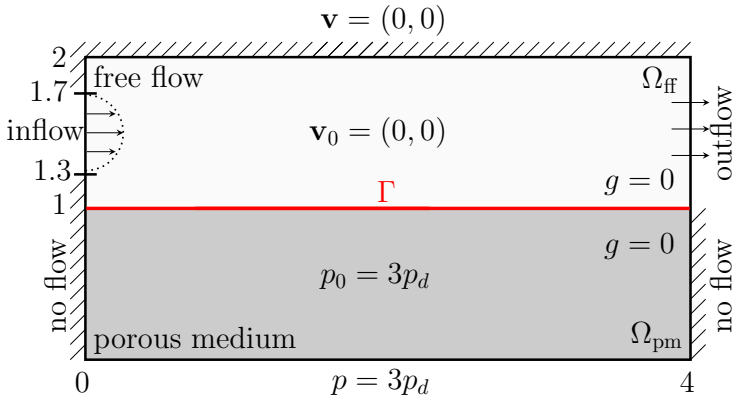

Fig. 8. Initial and boundary conditions for the realistic setup.

We consider the Brooks–Corey relative permeability-saturation relationship $k_r(S) = S_e^{3+\frac{2}{\lambda}}$, and the relationship between the effective saturation S_e and pressure

$$S_e(p) = \begin{cases} \left(\frac{p}{p_d}\right)^{-\lambda}, & p \le p_d, \\ 1, & p > p_d, \end{cases}$$

where the entry pressure is taken $p_d = -0.0136\,[\text{Pa}]$, and the Brooks–Corey parameter $\lambda = 1.09$. The saturation is computed as

$$S(p) = (S_{wm} - S_{wr})S_e(p) + S_{wr},$$

with the residual water-phase saturation $S_{wr} = 0.21$, and the maximum saturation $S_{wm} = 0.95$.

The initial and boundary conditions are described in Fig. 8. The inflow condition at the part of the left boundary of the free flow region $\partial\Omega_{\rm ff}^{\rm in} = \{0\} \times (1.3, 1.7\text{m})$ reads $u = 0.075 \arctan(2\pi t) \times \cos(\frac{\pi}{4})(y - \frac{1}{2})\,[\text{m/s}]$, $v = 0$, and the outflow condition at the right boundary of the free flow domain $\partial\Omega_{\rm ff}^{\rm out} = \{4\} \times (1, 2\text{m})$ is given by $\partial\mathbf{v}/\partial\mathbf{n} = 0$. At the remaining boundary of the free flow domain $\partial\Omega_{\rm ff} \setminus \left(\partial\Omega_{\rm ff}^{\rm in} \cup \partial\Omega_{\rm ff}^{\rm out} \cup \Gamma\right)$, zero fluid velocity $\mathbf{v} = (0, 0)$ is prescribed. At the left and right boundaries of the porous medium domain the no-flow conditions $\partial\widetilde{p}/\partial\mathbf{n} = 0$ are considered, and at the bottom boundary the pressure is specified as $p = 3p_d$. The initial free flow velocity is chosen to be zero, and the initial porous medium pressure is $p_0 = 3p_d$, which means that the porous medium is initially not fully saturated.

The porous medium is assumed to be fully saturated when the water-phase saturation becomes $S \geq 0.95$. Therefore, when this value is exceeded, only the water is considered to be present in the system, and instead of solving the non-stationary nonlinear equation (7), the stationary linear equation (8) is solved. These phase changes are dealt with inside the Newton loop and are updated in each iteration.

We choose $h = 0.04$, $\Delta t = 10^{-4}$, and $r = 5$. The time step is changing adaptively, depending on the convergence of the solver in the free flow domain and the number of the Newton iterations in the porous medium. When the residual of the free flow solution exceeds $\varepsilon_{\rm tol} = 10^{-10}$, or the number of the Newton steps in the porous medium region exceeds $N_{\rm tol} = 20$, then the time step is reduced $\Delta t_{\rm new} := 0.9\Delta t$. When both solvers demonstrate fast convergence behaviour, the time step is increased $\Delta t_{\rm new} := 1.02\Delta t$.

We plot the fluid velocity u in the free flow region (Fig. 9, upper subdomains) and the water-phase saturation S in the porous medium (Fig. 9, lower subdomains) at different times. Initially, the soil is saturated with 43% of water. In the beginning, mainly the inflow of water from the free flow region into the porous medium is observed (Fig. 9, top, middle). Then, when the upper layers of the soil system are fully saturated, the free fluid mainly flows out of the domain, and more and more porous medium layers become fully saturated (Fig. 9, bottom).

In Table 2, we present the time measurements and evaluate the efficiency of the decoupled algorithm. The results demonstrate the essential speedup of the multiple time-step scheme (Algorithm 1) applied for modeling realistic applications with phase changes.

Ratio r	1	2	5	10	20	30
CPU time, [s]	3838	2087	932	530	511	396
Speedup	1	1.84	4.12	7.24	7.51	9.69

Table 2
Speedup of Algorithm 1 for different time step ratios (realistic example).

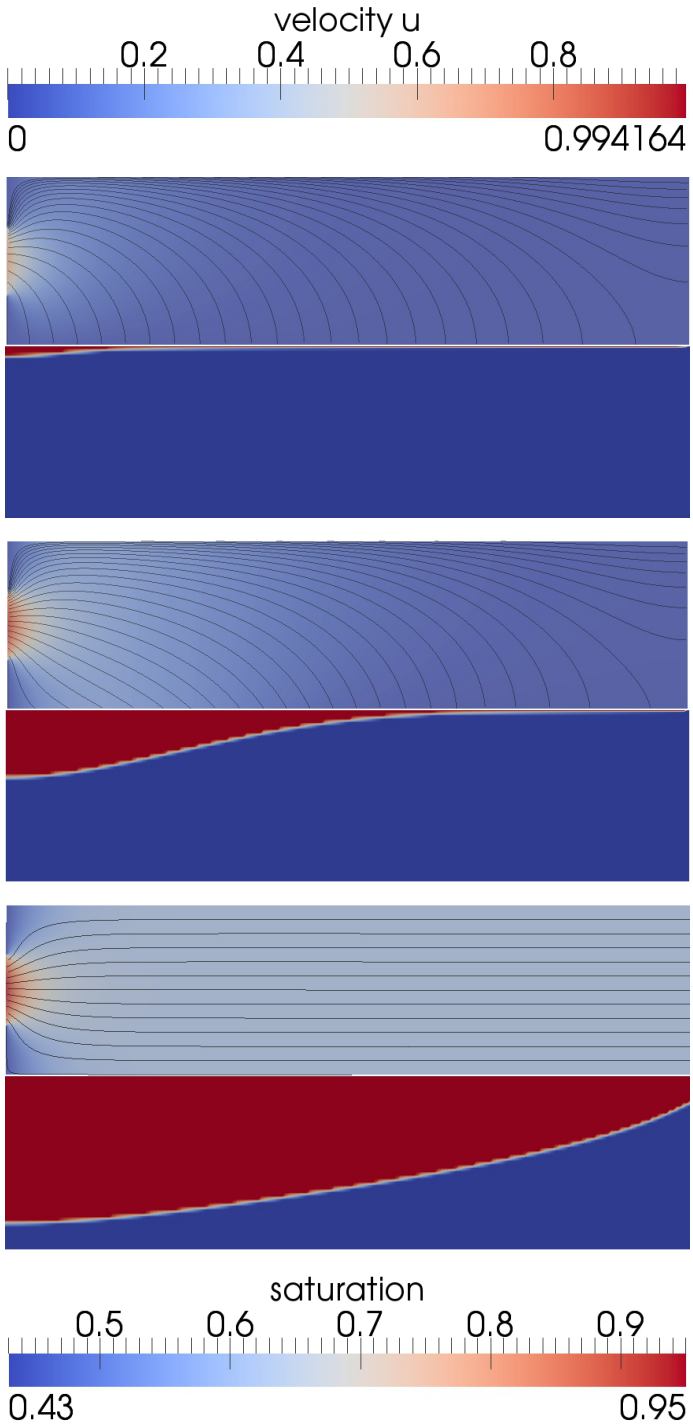

Fig. 9. Free flow velocity u and water-phase saturation S at $t = 0.5\,\mathrm{s}$ (top), $t = 2\,\mathrm{s}$ (middle), and $t = 5\,\mathrm{s}$ (bottom).

In Fig.10, we present the computational times spent on solving the coupled flow problem (red line), and the times spent on solving the Stokes equations (blue line) and the Richards equation (green line) separately for different ratios r. The total time needed to solve the free flow problem is reduced due to reuse of the factorizations at each coarse time interval.

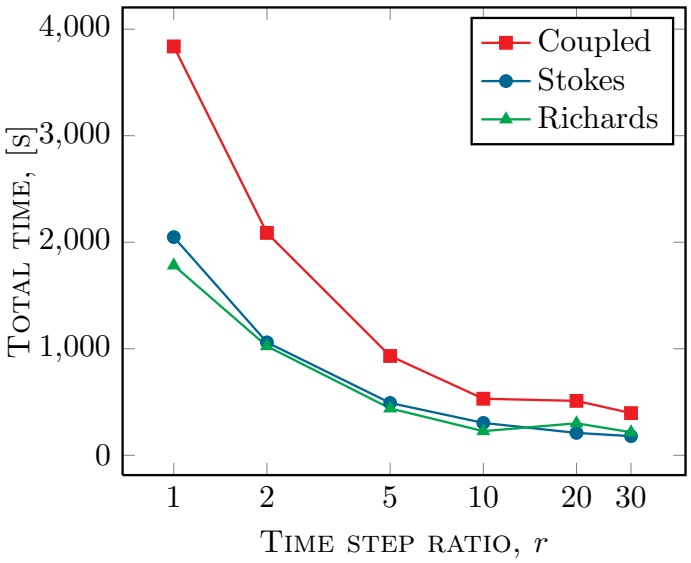

Fig. 10. Computational time reduction for different ratios r.

5 Discussion and conclusions

Due to increasing interest to simulations of interactions between the free flow and porous medium systems, the model formulations and numerical methods for their solution are of major importance. While the governing equations for the individual domains have been widely investigated, a challenge arises in accurate coupling of these flow models and development of efficient algorithms to solve these coupled problems.

For many environmental and industrial applications the physical processes in two subdomains evolve on different time scales. Therefore, the application of time-splitting schemes using different time steps (small step for fast solutions and large step for slow solutions) is an efficient alternative to conventional time-splitting methods typically used to solve such problems.

In this paper, we have coupled the Stokes equations and the Richards equation to describe fluid flow in the coupled free flow and variably saturated porous medium systems, and proposed a multiple-time-step scheme for efficient solution of such problems. Numerical simulations provided for the model problem with known analytical solution and for the realistic application demonstrate the convergence of the method and its efficiency.

Many extensions to the present work are possible: analysis of the time-splitting algorithm, development of different time-partitioning methods, considering higher order schemes, etc. From the modeling point of view, the full two-fluid-phase porous medium equations can be coupled with the free flow equations,

and transport of chemical species and energy can be taken into account. The proposed scheme seems to be especially efficient to model fluid flows in fractures where the solid matrix represents the porous medium system and the fracture network is treated as the free flow system.

Acknowledgments

This work was supported by German Research Foundation (DFG) project RY 126/2-1.

References

[1] Beavers, G., Joseph, D.: Boundary conditions at a naturally permeable wall. J. Fluid Mech. **30**, 197–207 (1967)

[2] Berninger, H., Ohlberger, M., Sander, O., Smetana, K.: Unsaturated subsurface flow with surface water and nonlinear in- and outflow conditions. Math. Models Methods Appl. Sci. **24**, 901–936 (2014)

[3] Caiazzo, A., John, V., Wilbrandt, U.: On classical iterative subdomain methods for the Stokes–Darcy problem. Comput. Geosci. (2014). DOI 10.1007/s10596-014-9418-y

[4] Cao, Y., Gunzburger, M., Hua, F., Wang, X.: Coupled Stokes–Darcy model with Beavers–Joseph interface boundary condition. Commun. Math. Sci. **8**, 1–25 (2010)

[5] Çeşmelioğlu, A., Rivière, B.: Primal discontinuous Galerkin methods for time-dependent coupled surface and subsurface flow. J. Sci. Comput. **40**, 115–140 (2009)

[6] Cimolin, F., Discacciati, M.: Navier–Stokes/Forchheimer models for filtration through porous media. Appl. Numer. Math. **72**, 205–224 (2013)

[7] Dawson, C.: A continuous/discontinuous Galerkin framework for modeling coupled subsurface and surface water flow. Comput. Geosci. **12**, 451–472 (2008)

[8] Discacciati, M., Miglio, E., Quarteroni, A.: Mathematical and numerical models for coupling surface and groundwater flows. Appl. Num. Math. **43**, 57–74 (2002)

[9] Discacciati, M., Quarteroni, A.: Navier–Stokes/Darcy coupling: modeling, analysis, and numerical approximation. Rev. Mat. Complut. **22**, 315–426 (2009)

[10] Hassanizadeh, S., Gray, W.: Boundary and interface conditions in porous media. Water Resour. Res. **25**, 1705–1715 (1989)

[11] Heroux, M., Bartlett, R., Hoekstra, V., Hu, J., Kolda, T., Lehoucq, R., Long, K., Pawlowski, R., Phipps, E., Salinger, A., Thornquist, H., Tuminaro, R., Willenbring, J., Williams, A.: An overview of Trilinos. Tech. Rep. SAND2003-2927, Sandia National Laboratories (2003)

[12] Kollet, S., Maxwell, R.: Integrated surface–groundwater flow modeling: A free-surface overland flow boundary condition in a parallel groundwater flow model. Adv. Water Res. **29**, 945–958 (2006)

[13] Layton, W., Tran, H., Trenchea, C.: Analysis of long time stability and errors of two partitioned methods for uncoupling evolutionary groundwater - surface water flows. SIAM J. Numer. Anal. **51**, 248–272 (2013)

[14] Layton, W., Tran, H., Xiong, X.: Long time stability of four methods for splitting the evolutionary Stokes–Darcy problem into Stokes and Darcy subproblems. J. Comput. Appl. Math. **236**, 3198–3217 (2012)

[15] Li, X.: An overview of SuperLU: algorithms, implementation, and user interface. ACM Trans. Math. Software **31**, 302–325 (2005)

[16] Mosthaf, K., Baber, K., Flemisch, B., Helmig, R., Leijnse, A., Rybak, I., Wohlmuth, B.: A coupling concept for two-phase compositional porous-medium and single-phase compositional free flow. Water Resour. Res. **47**, W10,522 (2011)

[17] Mu, M., Zhu, X.: Decoupled schemes for a non-stationary mixed Stokes–Darcy model. Math. Comp. **79**, 707–731 (2010)

[18] Ochoa-Tapia, A., Whitaker, S.: Momentum transfer at the boundary between a porous medium and a homogeneous fluid. I: Theoretical development. Int. J. Heat Mass Transfer **38**, 2635–2646 (1995)

[19] Richards, L.: Capillary conduction of liquids through porous mediums. J. Appl. Phys. **1**, 318–333 (1931)

[20] Rivière, B., Yotov, I.: Locally conservative coupling of Stokes and Darcy flow. SIAM J. Numer. Anal. **42**, 1959–1977 (2005)

[21] Rybak, I., Magiera, J.: A multiple-time-step technique for coupled free flow and porous medium systems. J. Comput. Phys. **272**, 327–342 (2014)

[22] Rybak, I., Magiera, J.: Decoupled schemes for free flow and porous medium systems. In: Domain Decomposition Methods in Science and Engineering XXII. Springer (in press)

[23] Shan, L., Zheng, H., Layton, W.: A decoupling method with different subdomain time steps for the nonstationary Stokes–Darcy model. Numer. Methods Partial Differential Equations **29**, 549–583 (2013)

[24] Shavit, U.: Special issue on "Transport phenomena at the interface between fluid and porous domains". Transp. Porous Media **78**, 327–330 (2009)

[25] Sochala, P., Ern, A., Piperno, S.: Mass conservative BDF-discontinuous Galerkin/explicit finite volume schemes for coupling subsurface and overland flows. Comput. Methods Appl. Mech. Engrg. **198**, 2122–2136 (2009)

[26] Sulis, M., Meyerhoff, S., Paniconi, C., Maxwell, R., Putti, M., Kollet, S.: A comparison of two physics-based numerical models for simulating surface water–groundwater interactions. Adv. Water Res. **33**, 456–467 (2010)

[27] Vassilev, D., Yotov, I.: Coupling Stokes–Darcy flow with transport. SIAM J. Sci. Comput. **31**, 3661–3684 (2009)

[28] Versteeg, H., Malalasekra, W.: An introduction to computational fluid dynamics: The finite volume method. Prentice Hall (2007)

Iryna Rybak
Pfaffenwaldring 57
70569 Stuttgart
Germany
E-Mail: rybak@ians.uni-stuttgart.de
WWW: http://www.mathematik.uni-stuttgart.de/fak8/ians/lehrstuhl/LstAngMath/mitarbeiter/rybak/

Jim Magiera
Pfaffenwaldring 57
70569 Stuttgart
Germany
E-Mail: magierjm@mathematik.uni-stuttgart.de

Rainer Helmig
Pfaffenwaldring 61
70569 Stuttgart
Germany
E-Mail: rainer.helmig@iws.uni-stuttgart.de
WWW: http://www.hydrosys.uni-stuttgart.de/institut/mitarbeiter/person.php?name=21

Christian Rohde
Pfaffenwaldring 57
70569 Stuttgart
Germany
E-Mail: crohde@mathematik.uni-stuttgart.de
WWW: http://www.mathematik.uni-stuttgart.de/fak8/ians/lehrstuhl/LstAngMath/mitarbeiter/rohde

Erschienene Preprints ab Nummer 2007/2007-001

Komplette Liste: `http://www.mathematik.uni-stuttgart.de/preprints`

2014-016 *Rybak, I.; Magiera, J.; Helmig, R.; Rohde, C.:* Multirate time integration for coupled saturated/unsaturated porous medium and free flow systems

2014-015 *Gaspoz, F.D.; Heine, C.-J.; Siebert, K.G.:* Optimal Grading of the Newest Vertex Bisection and H^1-Stability of the L_2-Projection

2014-014 *Kohler, M.; Krzyżak, A.; Walk, H.:* Nonparametric recursive quantile estimation

2014-013 *Kohler, M.; Krzyżak, A.; Tent, R.; Walk, H.:* Nonparametric quantile estimation using importance sampling

2014-012 *Györfi, L.; Ottucsák, G.; Walk, H.:* The growth optimal investment strategy is secure, too.

2014-011 *Györfi, L.; Walk, H.:* Strongly consistent detection for nonparametric hypotheses

2014-010 *Köster, I.:* Finite Groups with Sylow numbers $\{q^x, a, b\}$

2014-009 *Kahnert, D.:* Hausdorff Dimension of Rings

2014-008 *Steinwart, I.:* Measuring the Capacity of Sets of Functions in the Analysis of ERM

2014-007 *Steinwart, I.:* Convergence Types and Rates in Generic Karhunen-Loève Expansions with Applications to Sample Path Properties

2014-006 *Steinwart, I.; Pasin, C.; Williamson, R.; Zhang, S.:* Elicitation and Identification of Properties

2014-005 *Schmid, J.; Griesemer, M.:* Integration of Non-Autonomous Linear Evolution Equations

2014-004 *Markhasin, L.:* L_2- and $S^r_{p,q}B$-discrepancy of (order 2) digital nets

2014-003 *Markhasin, L.:* Discrepancy and integration in function spaces with dominating mixed smoothness

2014-002 *Eberts, M.; Steinwart, I.:* Optimal Learning Rates for Localized SVMs

2014-001 *Giesselmann, J.:* A relative entropy approach to convergence of a low order approximation to a nonlinear elasticity model with viscosity and capillarity

2013-016 *Steinwart, I.:* Fully Adaptive Density-Based Clustering

2013-015 *Steinwart, I.:* Some Remarks on the Statistical Analysis of SVMs and Related Methods

2013-014 *Rohde, C.; Zeiler, C.:* A Relaxation Riemann Solver for Compressible Two-Phase Flow with Phase Transition and Surface Tension

2013-013 *Moroianu, A.; Semmelmann, U.:* Generalized Killling spinors on Einstein manifolds

2013-012 *Moroianu, A.; Semmelmann, U.:* Generalized Killing Spinors on Spheres

2013-011 *Kohls, K; Rösch, A.; Siebert, K.G.:* Convergence of Adaptive Finite Elements for Control Constrained Optimal Control Problems

2013-010 *Corli, A.; Rohde, C.; Schleper, V.:* Parabolic Approximations of Diffusive-Dispersive Equations

2013-009 *Nava-Yazdani, E.; Polthier, K.:* De Casteljau's Algorithm on Manifolds

2013-008 *Bächle, A.; Margolis, L.:* Rational conjugacy of torsion units in integral group rings of non-solvable groups

2013-007 *Knarr, N.; Stroppel, M.J.:* Heisenberg groups over composition algebras

2013-006 *Knarr, N.; Stroppel, M.J.:* Heisenberg groups, semifields, and translation planes

2013-005 *Eck, C.; Kutter, M.; Sändig, A.-M.; Rohde, C.:* A Two Scale Model for Liquid Phase Epitaxy with Elasticity: An Iterative Procedure

2013-004 *Griesemer, M.; Wellig, D.:* The Strong-Coupling Polaron in Electromagnetic Fields

2013-003 *Kabil, B.; Rohde, C.:* The Influence of Surface Tension and Configurational Forces on the Stability of Liquid-Vapor Interfaces

2013-002 *Devroye, L.; Ferrario, P.G.; Györfi, L.; Walk, H.:* Strong universal consistent estimate of the minimum mean squared error

2013-001 *Kohls, K.; Rösch, A.; Siebert, K.G.:* A Posteriori Error Analysis of Optimal Control Problems with Control Constraints

2012-018 *Kimmerle, W.; Konovalov, A.:* On the Prime Graph of the Unit Group of Integral Group Rings of Finite Groups II

2012-017 *Stroppel, B.; Stroppel, M.:* Desargues, Doily, Dualities, and Exceptional Isomorphisms

2012-016 *Moroianu, A.; Pilca, M.; Semmelmann, U.:* Homogeneous almost quaternion-Hermitian manifolds

2012-015 *Steinke, G.F.; Stroppel, M.J.:* Simple groups acting two-transitively on the set of generators of a finite elation Laguerre plane

2012-014 *Steinke, G.F.; Stroppel, M.J.:* Finite elation Laguerre planes admitting a two-transitive group on their set of generators

2012-013 *Diaz Ramos, J.C.; Dominguez Vázquez, M.; Kollross, A.:* Polar actions on complex hyperbolic spaces

2012-012 *Moroianu; A.; Semmelmann, U.:* Weakly complex homogeneous spaces

2012-011 *Moroianu; A.; Semmelmann, U.:* Invariant four-forms and symmetric pairs

2012-010 *Hamilton, M.J.D.:* The closure of the symplectic cone of elliptic surfaces

2012-009 *Hamilton, M.J.D.:* Iterated fibre sums of algebraic Lefschetz fibrations

2012-008 *Hamilton, M.J.D.:* The minimal genus problem for elliptic surfaces

2012-007 *Ferrario, P.:* Partitioning estimation of local variance based on nearest neighbors under censoring

2012-006 *Stroppel, M.:* Buttons, Holes and Loops of String: Lacing the Doily

2012-005 *Hantsch, F.:* Existence of Minimizers in Restricted Hartree-Fock Theory

2012-004 *Grundhöfer, T.; Stroppel, M.; Van Maldeghem, H.:* Unitals admitting all translations

2012-003 *Hamilton, M.J.D.:* Representing homology classes by symplectic surfaces

2012-002 *Hamilton, M.J.D.:* On certain exotic 4-manifolds of Akhmedov and Park

2012-001 *Jentsch, T.:* Parallel submanifolds of the real 2-Grassmannian

2011-028 *Spreer, J.:* Combinatorial 3-manifolds with cyclic automorphism group

2011-027 *Griesemer, M.; Hantsch, F.; Wellig, D.:* On the Magnetic Pekar Functional and the Existence of Bipolarons

2011-026 *Müller, S.:* Bootstrapping for Bandwidth Selection in Functional Data Regression

2011-025 *Felber, T.; Jones, D.; Kohler, M.; Walk, H.:* Weakly universally consistent static forecasting of stationary and ergodic time series via local averaging and least squares estimates

2011-024 *Jones, D.; Kohler, M.; Walk, H.:* Weakly universally consistent forecasting of stationary and ergodic time series

2011-023 *Györfi, L.; Walk, H.:* Strongly consistent nonparametric tests of conditional independence

2011-022 *Ferrario, P.G.; Walk, H.:* Nonparametric partitioning estimation of residual and local variance based on first and second nearest neighbors

2011-021 *Eberts, M.; Steinwart, I.:* Optimal regression rates for SVMs using Gaussian kernels

2011-020 *Frank, R.L.; Geisinger, L.:* Refined Semiclassical Asymptotics for Fractional Powers of the Laplace Operator

2011-019 *Frank, R.L.; Geisinger, L.:* Two-term spectral asymptotics for the Dirichlet Laplacian on a bounded domain

2011-018 *Hänel, A.; Schulz, C.; Wirth, J.:* Embedded eigenvalues for the elastic strip with cracks

2011-017 *Wirth, J.:* Thermo-elasticity for anisotropic media in higher dimensions

2011-016 *Höllig, K.; Hörner, J.:* Programming Multigrid Methods with B-Splines

2011-015 *Ferrario, P.:* Nonparametric Local Averaging Estimation of the Local Variance Function

2011-014 *Müller, S.; Dippon, J.:* k-NN Kernel Estimate for Nonparametric Functional Regression in Time Series Analysis

2011-013 *Knarr, N.; Stroppel, M.:* Unitals over composition algebras

2011-012 *Knarr, N.; Stroppel, M.:* Baer involutions and polarities in Moufang planes of characteristic two

2011-011 *Knarr, N.; Stroppel, M.:* Polarities and planar collineations of Moufang planes

2011-010 *Jentsch, T.; Moroianu, A.; Semmelmann, U.:* Extrinsic hyperspheres in manifolds with special holonomy

2011-009 *Wirth, J.:* Asymptotic Behaviour of Solutions to Hyperbolic Partial Differential Equations

2011-008 *Stroppel, M.:* Orthogonal polar spaces and unitals

2011-007 *Nagl, M.:* Charakterisierung der Symmetrischen Gruppen durch ihre komplexe Gruppenalgebra

2011-006 *Solanes, G.; Teufel, E.:* Horo-tightness and total (absolute) curvatures in hyperbolic spaces

2011-005 *Ginoux, N.; Semmelmann, U.:* Imaginary Kählerian Killing spinors I

2011-004 *Scherer, C.W.; Köse, I.E.:* Control Synthesis using Dynamic D-Scales: Part II — Gain-Scheduled Control

2011-003 *Scherer, C.W.; Köse, I.E.:* Control Synthesis using Dynamic D-Scales: Part I — Robust Control

2011-002 *Alexandrov, B.; Semmelmann, U.:* Deformations of nearly parallel G_2-structures

2011-001 *Geisinger, L.; Weidl, T.:* Sharp spectral estimates in domains of infinite volume

2010-018 *Kimmerle, W.; Konovalov, A.:* On integral-like units of modular group rings

2010-017 *Gauduchon, P.; Moroianu, A.; Semmelmann, U.:* Almost complex structures on quaternion-Kähler manifolds and inner symmetric spaces

2010-016 *Moroianu, A.; Semmelmann,U.:* Clifford structures on Riemannian manifolds

2010-015 *Grafarend, E.W.; Kühnel, W.:* A minimal atlas for the rotation group $SO(3)$

2010-014 *Weidl, T.:* Semiclassical Spectral Bounds and Beyond

2010-013 *Stroppel, M.:* Early explicit examples of non-desarguesian plane geometries

2010-012 *Effenberger, F.:* Stacked polytopes and tight triangulations of manifolds

2010-011 *Györfi, L.; Walk, H.:* Empirical portfolio selection strategies with proportional transaction costs

2010-010 *Kohler, M.; Krzyżak, A.; Walk, H.:* Estimation of the essential supremum of a regression function

2010-009 *Geisinger, L.; Laptev, A.; Weidl, T.:* Geometrical Versions of improved Berezin-Li-Yau Inequalities

2010-008 *Poppitz, S.; Stroppel, M.:* Polarities of Schellhammer Planes

2010-007 *Grundhöfer, T.; Krinn, B.; Stroppel, M.:* Non-existence of isomorphisms between certain unitals

2010-006 *Höllig, K.; Hörner, J.; Hoffacker, A.:* Finite Element Analysis with B-Splines: Weighted and Isogeometric Methods

2010-005 *Kaltenbacher, B.; Walk, H.:* On convergence of local averaging regression function estimates for the regularization of inverse problems

2010-004 *Kühnel, W.; Solanes, G.:* Tight surfaces with boundary

2010-003 *Kohler, M; Walk, H.:* On optimal exercising of American options in discrete time for stationary and ergodic data

2010-002 *Gulde, M.; Stroppel, M.:* Stabilizers of Subspaces under Similitudes of the Klein Quadric, and Automorphisms of Heisenberg Algebras

2010-001 *Leitner, F.:* Examples of almost Einstein structures on products and in cohomogeneity one

2009-008 *Griesemer, M.; Zenk, H.:* On the atomic photoeffect in non-relativistic QED

2009-007 *Griesemer, M.; Moeller, J.S.:* Bounds on the minimal energy of translation invariant n-polaron systems

2009-006 *Demirel, S.; Harrell II, E.M.:* On semiclassical and universal inequalities for eigenvalues of quantum graphs

2009-005 *Bächle, A, Kimmerle, W.:* Torsion subgroups in integral group rings of finite groups

2009-004 *Geisinger, L.; Weidl, T.:* Universal bounds for traces of the Dirichlet Laplace operator

2009-003 *Walk, H.:* Strong laws of large numbers and nonparametric estimation

2009-002 *Leitner, F.:* The collapsing sphere product of Poincaré-Einstein spaces

2009-001 *Brehm, U.; Kühnel, W.:* Lattice triangulations of E^3 and of the 3-torus

2008-006 *Kohler, M.; Krzyżak, A.; Walk, H.:* Upper bounds for Bermudan options on Markovian data using nonparametric regression and a reduced number of nested Monte Carlo steps

2008-005 *Kaltenbacher, B.; Schöpfer, F.; Schuster, T.:* Iterative methods for nonlinear ill-posed problems in Banach spaces: convergence and applications to parameter identification problems

2008-004 *Leitner, F.:* Conformally closed Poincaré-Einstein metrics with intersecting scale singularities

2008-003 *Effenberger, F.; Kühnel, W.:* Hamiltonian submanifolds of regular polytope

2008-002 *Hertweck, M.; Höfert, C.R.; Kimmerle, W.:* Finite groups of units and their composition factors in the integral group rings of the groups $PSL(2,q)$

2008-001 *Kovarik, H.; Vugalter, S.; Weidl, T.:* Two dimensional Berezin-Li-Yau inequalities with a correction term

2007-006 *Weidl, T.:* Improved Berezin-Li-Yau inequalities with a remainder term

2007-005 *Frank, R.L.; Loss, M.; Weidl, T.:* Polya's conjecture in the presence of a constant magnetic field

2007-004 *Ekholm, T.; Frank, R.L.; Kovarik, H.:* Eigenvalue estimates for Schrödinger operators on metric trees

2007-003 *Lesky, P.H.; Racke, R.:* Elastic and electro-magnetic waves in infinite waveguides

2007-002 *Teufel, E.:* Spherical transforms and Radon transforms in Moebius geometry

2007-001 *Meister, A.:* Deconvolution from Fourier-oscillating error densities under decay and smoothness restrictions